Band structure of one-dimensional plasma photonic crystals using the Fresnel coefficients method

A. Jafari & A. Rahmat

Indian Journal of Physics

ISSN 0973-1458

Indian J Phys
DOI 10.1007/s12648-016-0934-6

Springer

Indian J Phys
DOI 10.1007/s12648-016-0934-6

ORIGINAL PAPER

Band structure of one-dimensional plasma photonic crystals using the Fresnel coefficients method

A Jafari* and A Rahmat

Atomic and Molecular Group, Faculty of Science, Urmia University, Urmia, Iran

Received: 22 February 2016 / Accepted: 16 September 2016

Abstract: The current study has examined the band structures of two types of photonic crystals (PCs). The first is a one-dimensional metamaterial photonic crystal (1DMMPC) composed of double-layered units for which both layers of each unit are dielectric. The second type is a very similar one-dimensional plasma photonic crystal (1DPPC) also composed of double-layered units in which the first layer is a dielectric material but the second is a plasma layer. This study compares the band structures of the 1DMMPC with specific optical characteristics of the 1DPPC using the Fresnel coefficients method and also compares the results of this method with the results of the transfer matrix method. It is concluded that the dependency of the electric permittivity of the plasma layer on the incident field frequency causes differences in the band structures in 1DMMPC and 1DPPC for both TE and TM polarizations and their gaps reside in different frequencies. The band structures of the 1DMMPC and 1DPPC are confirmed by the results of the transfer matrix method.

Keywords: Band structure; Plasma photonic crystal; Fresnel coefficient; Plasma layer; Metamaterial photonic crystal; 100% reflection

PACS Nos.: 42.70.Qs; 78.20.Ci; 41.20.Jb; 78.67.Pt

1. Introduction

Photonic crystals (PCs) are composed of periodic dielectric layers that affect the propagation of electromagnetic waves in a way similar to how a periodic potential affects electrons in semiconductors. Metamaterials (MMs) are a new class of materials that possess a negative index of refraction. In fact, PCs are regularly repetitive regions with different dielectric layers. The wavelength that can be propagated within the crystal is known as the mode. The allowed mode groups create bands. Forbidden bands are called PC band gap wavelengths.

PCs can be fabricated in one, two or three dimensions. One-dimensional (1D) PCs can be made of layers deposited on or stuck to other layers. Two-dimensional PCs can be made through photolithography or by drilling holes in a suitable substrate. Fabrication methods for three-dimensional PCs include drilling at different angles and stacking multiple 2D layers on top of one another [1–5]. The interest in PC band gaps stems from their application in research and technology such as filters, waveguides, optical switches and cavities [6–11].

The PC concept was proposed by Yablonovitch [12] and John [13] in 1987. Recently, PCs have been extended to plasma photonic crystals (PPCs). The PPC concept was initially proposed by Hojo [14]. These types of PCs are either composed of periodic layers of microplasma and dielectric materials or of microplasma layers with periodic density distributions that have specific characteristics that differ from those of metamaterial photonic crystals (MMPCs).

Plasma is a dispersive material with a refractive index that is dependent on the incident electromagnetic wave frequency and follows the Drude model. The refractive index of unmagnetized plasma is determined by the frequencies of the electromagnetic wave and the plasma. The permittivity of plasma can be tuned to a specific amount by changing the electromagnetic wave and plasma frequencies. This characteristic of PPCs separates them from MMPCs and conventional PCs [15–18]. Characteristics of MMPC and PPC band structures were previously surveyed using the transfer matrix method. A few points on omnidirectional band gaps in 1D PCs were provided [19].

*Corresponding author, E-mail: a.jafari@urmia.ac.ir

Published online: 12 November 2016

Differential transfer matrix method for photonic band structure of 1D non-uniform distribution PPCs was discussed [20]. photonic band structure solved by a plane-wave-based transfer-matrix method was carried out [21]. Ultra-wide low-frequency band gap of 1D superconducting PCs containing MMs was investigated [22]. Zero permeability and zero permittivity band gaps in 1D MMPCs were studied [23] and the omnidirectional gap and defect mode of 1D PCs with single-negative materials were studied [24].

The current study has examined the band structures of one-dimensional metamaterial photonic crystals (1DMMPCs) and one-dimensional plasma photonic crystals (1DPPCs) calculated using the Fresnel coefficients method. Other than a second layer substitution of plasma in their double-layered dielectrics, 1DPPCs exhibit the characteristics of 1DMMPCs. The study had two goals. The first was to calculate the band structures of 1DMMPCs using the Fresnel coefficients method and compare them with the results of the transfer matrix method. The second was to survey the band structures of these MMPCs with a plasma layer. It was observed that the results of the Fresnel coefficients method were confirmed by the transfer matrix method [23, 24].

The permittivity and permeability of the MMPCs depended on the incident field frequency and did not follow the Drude model [23, 24]. The purpose of selecting these crystal types is that they possess different optical properties and their band structures, which were acquired using the transfer matrix method, have been cited in aforementioned studies. The diagrams acquired in the present study through the Fresnel coefficients method were confirmed by these studies.

Section 2 discusses the basic considerations of the Fresnel coefficient method for calculating the band structure of PCs. Section 3 calculates and compares the band structures of the two types of MMPCs to their corresponding types of PPCs. The paper concludes in Sect. 4.

2. Basic consideration

In the calculation of PC band structure, the refractive indices of each layer of slab and the initial incident light angle are used to acquire the Fresnel coefficients. These coefficients can be used to determine the transmission and reflection coefficients of the crystal along with the necessary and sufficient conditions for 100% reflection from its surface. In fact, using these equations, there is a tendency of the reflection coefficient to be unitary; therefore, the band structure of the PC can be determined [16, 25–27].

Consider a periodic multilayer stack as depicted in Fig. 1 where, r, r' and t are the reflection coefficients of the upper and lower layers and the transmission coefficient of each layer, respectively. δ is the phase delay from the existence of an air gap between the first and other layers of the crystal and r_0 is the total reflection coefficient from the lower layers (excluding the upper layer). Considering the amplitude and phase of the quantities gives [26, 27]:

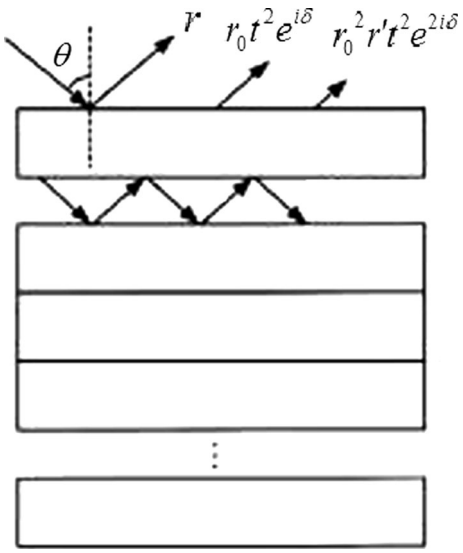

Fig. 1 Calculation of periodic stack reflection coefficient, r_0, in terms of the individual block parameters r, r' and t

$$r_0 = |r_0|e^{i\phi_0}, \quad r' = |r'|e^{i\phi_{r'}}, \quad r = |r|e^{i\phi_r} \tag{1}$$

$$\frac{1}{2}(\phi_r + \phi_{r'}) = \phi_t \pm \frac{\pi}{2} \tag{2}$$

where, ϕ_r and $\phi_{r'}$ are the phase shifts upon reflection of the upper and lower layers, respectively, and ϕ_t is the phase shift upon transmission in each layer. From Fig. 1, r_0 can be calculated as:

$$r_0 = \frac{r - r_0(rr' - t^2)}{1 - r_0 r'} \tag{3}$$

According to the reciprocal properties of electromagnetic waves in non-absorbing media, t should be the same whether the incidence is from the top or bottom, as in this case where $|r| = |r'|$ and $|r|^2 + |t|^2 = 1$. Substituting Eqs. (1) and (2) into Eq. (3) obtains:

$$\cos\left[\phi_0 - {}^1\!/_2(\phi_r - \phi_{r'})\right] = \frac{\cos\left[\frac{1}{2}(\phi_r + \phi_{r'})\right]}{|r|} \tag{4}$$

Because the right-hand-side of Eq. (4) is confined to interval $[-1, +1]$; considering the mathematical calculation needed for 100% reflection from the crystal surface, $|r_0| = 1$, leads to the following important inequalities [26]:

$$|t| < |\cos(\phi_t)| \tag{5}$$

$$|r| > |\sin(\phi_t)| \tag{6}$$

The goal is to calculate the band structure of 1D PCs composed of double-layered dielectrics. The transmission coefficient and conditions of 100% reflection from the surface should be calculated.

2.1. Calculation of transmission and conditions for 100% reflection from surface of double-layered dielectrics

Consider a dielectric composed of two layers. In Fig. 2, n_1, d_1, t_1, r_1 are the refractive index, thickness, transmission, and reflection coefficients of the upper layer, respectively, and n_2, d_2, t_2, r_2 are the corresponding parameters of the second layer. Figure 2 gives:

$$t = t_1 t_2 + t_1 t_2 r_1 r_2 + t_1 t_2 r_1^2 r_2^2 + \ldots \tag{7}$$

Using the magnitude and phase of the quantities in Eq. (7) with some simplification gives:

$$|t| = \frac{|t_1||t_2|}{\sqrt{1 + (|r_1||r_2|)^2 - 2|r_1||r_2|\cos(\phi_{r_1} + \phi_{r_2})}} \tag{8}$$

$$\phi_t = \tan^{-1}\left[\frac{\sin(\phi_{t_1} + \phi_{t_2})}{\cos(\phi_{r_1} + \phi_{r_2}) + |r_1||r_2|}\right] \tag{9}$$

In which $|t_1|, |t_2|, |r_1|, |r_2|, \phi_{r_1}, \phi_{r_2}$ are the transmission, reflection and phase of the reflection of a single layer dielectric and can be written as [26]:

$$|r| = \frac{2\rho \sin\Delta}{\sqrt{\rho^4 - 2\rho^2 \cos 2\Delta + 1}} \tag{10}$$

$$\phi_r = \tan^{-1}\left[\frac{1-\rho^2}{(1+\rho^2)\tan\Delta}\right] \tag{11}$$

$$|t| = \frac{1-\rho^2}{\sqrt{\rho^4 - 2\rho^2 \cos 2\Delta + 1}} \tag{12}$$

In Eqs. (10), (11) and (12), Δ is the single- path phase shift and is defined as:

$$\Delta = 2\pi\left(\frac{d}{\lambda_0}\right)\sqrt{n^2 - \sin^2\theta} \tag{13}$$

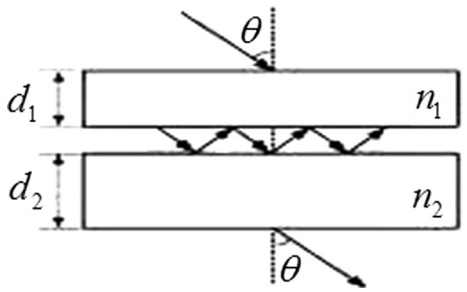

Fig. 2 Calculation of bilayer slab transmission coefficient, t, composed of two layers with optical characteristics n_1 and d_1 for upper layer and n_2 and d_2 for second layer

where ρ is the reflection coefficient from the dielectric upper layer and can be defined using the Fresnel coefficients for s and p polarizations [26, 27] as:

$$\rho_s = \frac{\cos\theta - \sqrt{n^2 - \sin^2\theta}}{\cos\theta + \sqrt{n^2 - \sin^2\theta}} \quad \rho_P = \frac{\sqrt{n^2 - \sin^2\theta} - n^2\cos\theta}{\sqrt{n^2 - \sin^2\theta} + n^2\cos\theta} \tag{14}$$

Using Eqs. (5), (6), (8), and (9) gives:

$$|t_1||t_2| < \left||r_1||r_2| - \cos(\phi_{r_1} + \phi_{r_2})\right| \tag{15}$$

Substituting Eqs. (10)–(12) into Inequality (15) obtains the two following important inequalities:

$$\frac{(\rho_1 - \rho_2)^2}{(1-\rho_1^2)(1-\rho_2^2)}\sin\Delta_1 \sin\Delta_2 > \cos^2\left(\frac{\Delta_1 + \Delta_2}{2}\right) \tag{16}$$

$$\frac{(\rho_1 - \rho_2)^2}{(1-\rho_1^2)(1-\rho_2^2)}\sin\Delta_1 \sin\Delta_2 < -\sin^2\left(\frac{\Delta_1 + \Delta_2}{2}\right) \tag{17}$$

Inequalities (16) and (17) are the necessary and sufficient conditions for calculating the band structure of PCs using the Fresnel coefficients. In this method no assumptions about the periodicity of the system and its consequences are made, unlike the transfer matrix method, which relies on the Bloch theorem. In the next section, the band structures of the MMPCs and PPCs are calculated and compared using the Fresnel coefficients and transfer matrix methods and are denoted in different colors and line fonts.

3. Results and discussion

3.1. Type 1 MMPC band structure with given optical characteristics

The optical characteristics of this MMPC are as follows:

$$\varepsilon_0 = \mu_0 = 1, \varepsilon_1 = 3, \varepsilon_2 = 1 - \left(\frac{\omega_{ep}}{\omega}\right)^2,$$

$$\mu_1 = 1 - \left(\frac{\omega_{mp}}{\omega}\right)^2, \mu_2 = 1.2, d_1 = 10\,\text{mm}, d_2 = 5\,\text{mm}$$

where $\omega_{ep} = 12GHz$, $\omega_{mp} = 10GHz$.

Using Inequalities (16) and (17), the band structures of this MMPC for both TE and TM polarizations are plotted using both methods in Fig. 3 and are distinguished by different colors and line fonts. In this figure,θ is the primary radiation angle toward the crystal surface.

From Figs. 3(a) and 3(b), it is clear that the results of both methods are the same and overlap [24]. Photonic band gap (PBG) structure is a substantial feature of PCs. The usual PBGs induced by Bragg scattering are called Bragg gaps. In the conventional PC, Bragg gaps are strongly dependent on the angle and polarization of the incident light. The "zero averaged index" gaps that appear in 1D

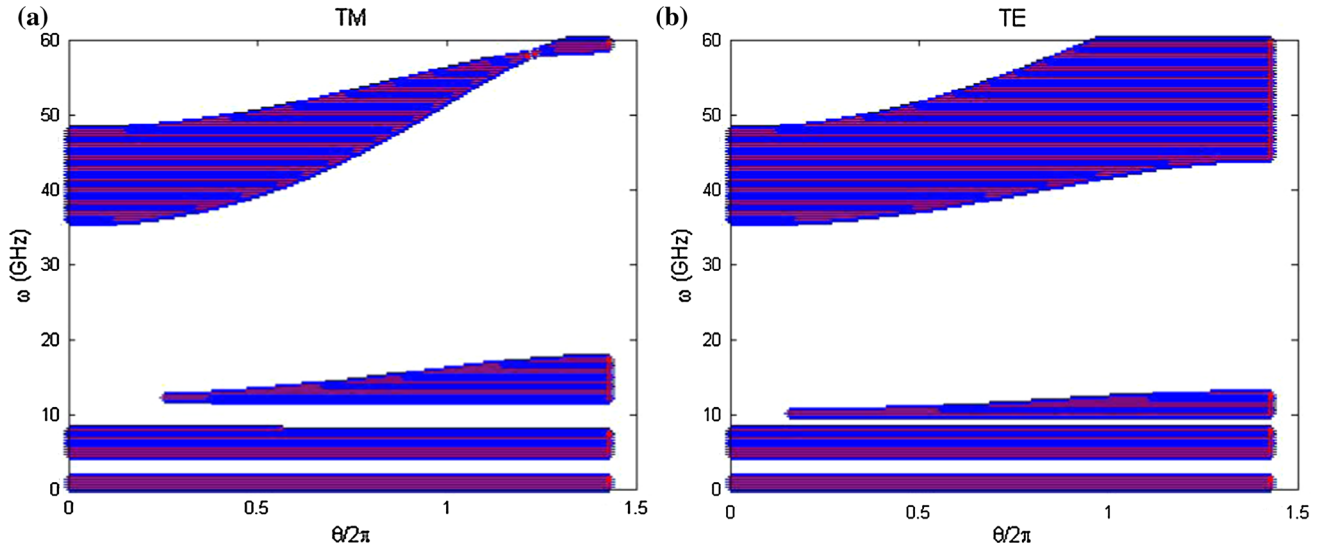

Fig. 3 Band structure of type 1 MMPCs by Fresnel coefficients method (*blue color*) and transfer matrix method (*red color*) for: (**a**) TM polarization and; (**b**) TE polarization (color figure online)

PCs and are composed of positive- and negative-index materials are independent of the angle and polarization of the incident light (omnidirectional gaps). Materials with $\varepsilon<0$ or $\mu<0$ are called single—negative (SNG) materials [28]. The PBGs are surrounded by the propagating modes. These modes are produced by the interaction of two eradicable waves in the SNG frequency range that propagate in opposite directions. These PBGs are called single—negative gaps. Materials with $\varepsilon<0$ and $\mu<0$ are called double—negative (DNG) materials [29–32]. In the type 1 MMPC, the SNG frequency range is determined by $\omega^2<\omega_{ep}^2, \omega_{mp}^2$ [33, 34].

In Fig. 3(a), the uppermost branch of the band structure diagram for TM polarization is called the Bragg gap and is dependent on the incident angle. As seen, the width of the Bragg gap decreases as the incident angle increases. The angular band gap beneath the uppermost branch is also dependent on the incident angle; the width of this band gap increases as the angle increases. The two lower branches are called omnidirectional band gaps because their widths remain the same as the angle varies.

The uppermost branch of the band structure diagram for TE polarization (Fig. 3(b)) is also called the Bragg gap; its width also increases as the angle increases. The area below the uppermost branch is called the angular band gap and the width of it increases as the angle increases. The two branches beneath the angular band gap are called omnidirectional band gaps; their widths remain constant as the angle varies [24].

The following example is a PPC composed of double-layered slabs. The first layer is a dielectric similar to a MMPC (type 1), but the second dielectric layer is replaced by a plasma layer.

3.2. Type 1 PPC band structure with given optical characteristics

For this type of PPC, the optical characteristics are:

$$\varepsilon_0=\mu_0=1, \varepsilon_1=3, \varepsilon_2=1-\frac{\omega_p^2}{\omega(\omega-i\upsilon)},$$

$$\mu_1=1-\left(\frac{\omega_{mp}}{\omega}\right)^2, \mu_2=1, d_1=10\ \text{mm}, d_2=5\ \text{mm}$$

$$\omega_p=8\pi\ \text{GHz}, \upsilon=3\ \text{GHz}, \omega_{mp}=10\ \text{GHz}$$

in which the plasma dielectric constant is $\varepsilon_2=\varepsilon_p(\omega)$ and follows the Drude model [35] and ω_p and υ are the plasma frequency and electron collision frequency, respectively.

Using Inequalities (16) and (17), the band structures of this PPC type are plotted for both TM and TE polarizations in Fig. 4 using different colors and line fonts. In this figure, θ is the primary radiation angle toward the crystal surface.

3.3. Type 2 MMPC band structure with given optical characteristics

The optical characteristics of this PC are as follows:

$$\varepsilon_0=\mu_0=1, \varepsilon_1=1, \varepsilon_2(f)=1+\frac{5^2}{0.9^2-f^2}+\frac{10^2}{11.5^2-f^2},$$

$$\mu_1=1$$

$$\mu_2(f)=1+\frac{3^2}{0.902^2-f^2}, \quad d_1=12\ mm, \quad d_2=6\ mm$$

where f is the frequency of the incident light (GHz). Substituting these characteristics into Inequalities (16) and (17) results in the diagram of the band structures in Fig. 5 for

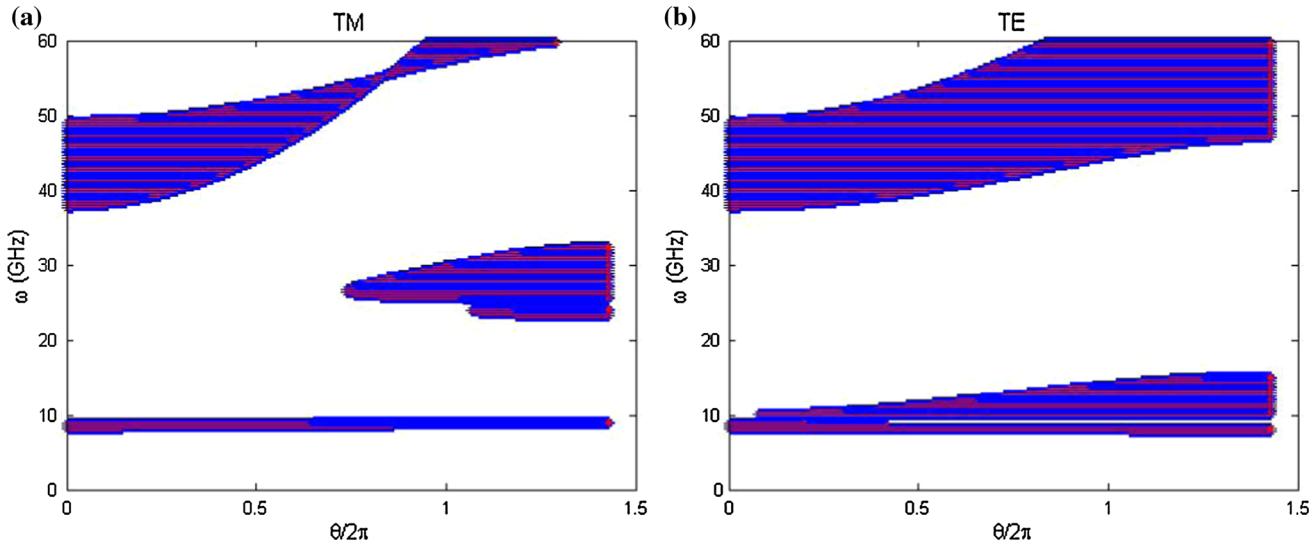

Fig. 4 Band structure of type 1 PPCs by Fresnel coefficients method (*blue color*) and transfer matrix method (*red color*) for: (**a**) TM polarization and; (**b**) TE polarization (color figure online)

both TE and TM polarizations denoted in different colors and line fonts. In this figure, θ is the primary radiation angle toward the crystal surface in terms of degrees.

It is known that at the frequencies in which the $\mu(\omega)$ or $\varepsilon(\omega)$ signs change, the refractive index of a MM becomes zero, and "zero averaged refractive index" gaps are found for both TE and TM polarizations. When $\mu = 0$, a gap appears in the band structure of the PCs for TE polarization and when $\varepsilon = 0$, a gap appears in the band structure of the PCs for TM polarization [33, 36–38]. These gaps, which depend on the incident angle of the light, can be observed in some PCs [33].

Figures 6(a) and 6(b) show the plots of μ_2 and ε_2 as a function of frequency, respectively.

As seen, μ_2 and ε_2 acquired null values at $f \approx 3$ GHz and $f \approx 4$ GHz, respectively. This is confirmed by Figs. 5(a) and 5(b), in which $f \approx 3$ GHz and $f \approx 4$ *GHz* are the initial frequencies of the branch band gaps related to $\mu = 0$ and $\varepsilon = 0$, respectively.

It can be seen in Figs. 4 and 5 that the results of both methods are the same and overlap [23]. In Figs. 5(a) and 5(b), the lowest branch of the diagram is related to "zero averaged refractive index" for which increasing the angle in TM polarization decreases the width. For TE

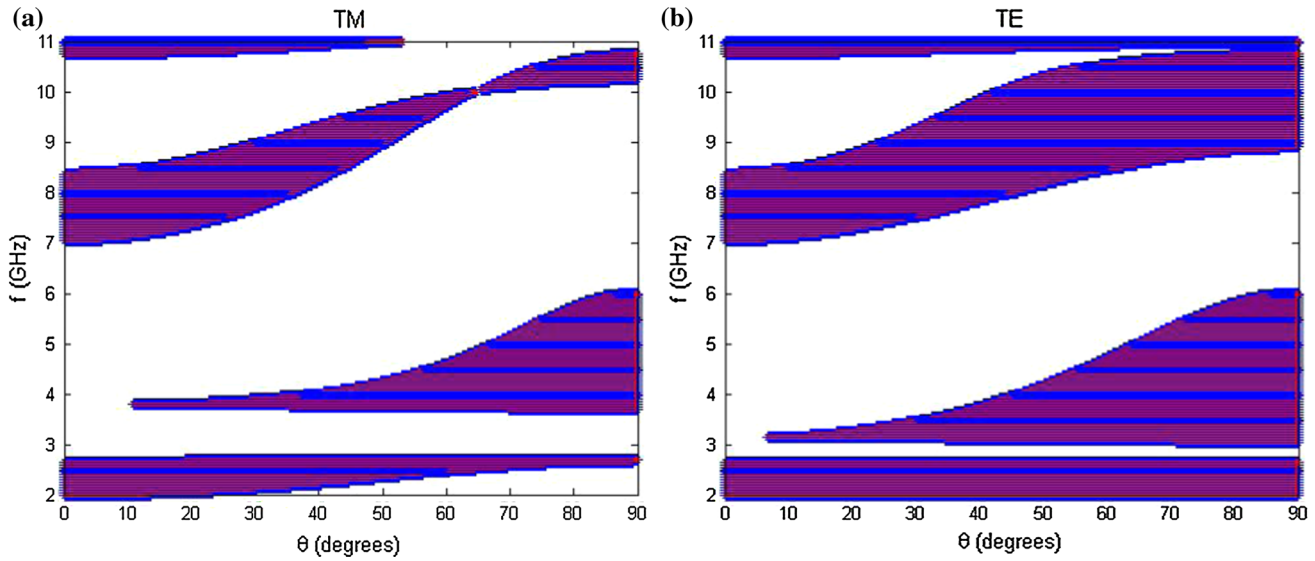

Fig. 5 Band structure of type 2 MMPCs by Fresnel coefficients method (*blue color*) and transfer matrix method (*red color*) for: (**a**) TM polarization and; (**b**) TE polarization (color figure online)

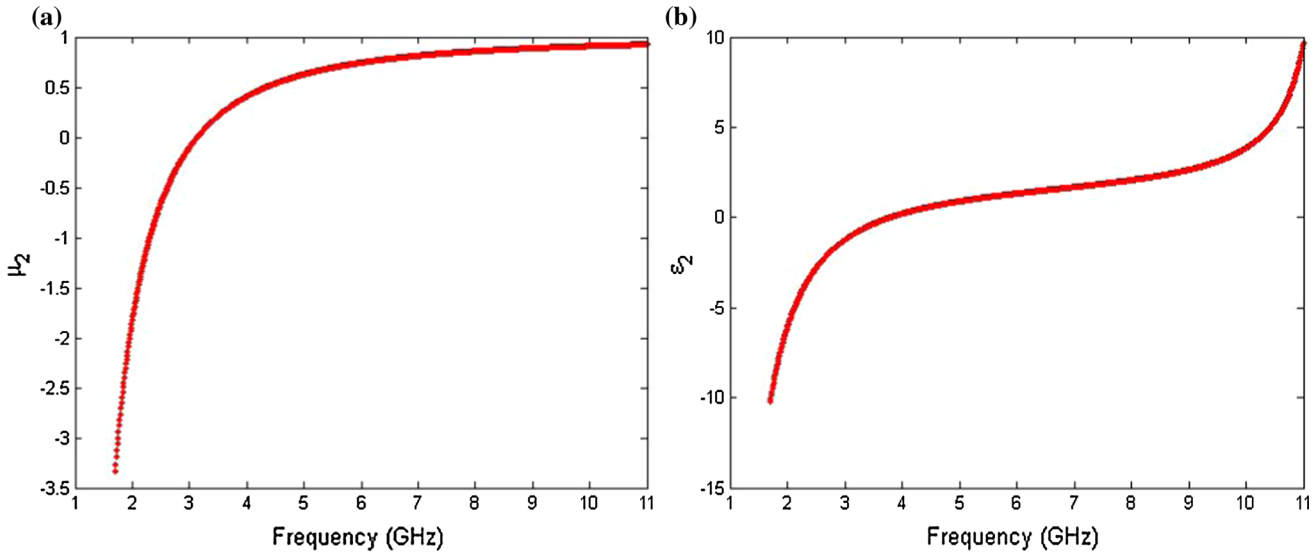

Fig. 6 Diagram in terms of frequency for: (**a**) μ_2 and; (**b**)ε_2

polarization in Fig. 5(b), which is independent of angle variation, the width remains constant.

The branch below the uppermost gap relates to permeability and permittivity. In TM polarization, it is related to "zero permittivity". Increasing the angle at this polarization increases the width of the band gap. In TE polarization, this gap does not exist; instead, there is a band gap related to "zero permeability" for which increasing the angle increases the width. The uppermost branch of these gaps is related to the Bragg band gap; as the angle in TM polarization increases, the width initially decreases and then begins to increase. For TE polarization, the width increases as the angle increases [23]. The band structures of type 2 PPCs are calculated below.

3.4. Type 2 PPC band structure with given optical characteristics

The optical characteristics for this PPC are:

$$\varepsilon_0 = \mu_0 = 1, \varepsilon_1 = 1, \varepsilon_2(f) = 1 - \frac{\omega_p^2}{\omega(\omega - i\upsilon)}, \mu_1 = 1$$

$$\mu_2 = 1, \quad d_1 = 12\ mm, \quad d_2 = 6\ mm$$

where $\upsilon = 3$ GHz, $\omega_p = 8\pi$ GHz and f is the incident field frequency in terms of GHz. The band structures for both TE and TM polarizations are plotted in Fig. 7 in different colors and line fonts. In this figure, θ is the primary radiation angle toward the crystal surface in terms of degrees.

As seen in Figs. 3(a) and 4(a), the lower omnidirectional branch of the band gap has been omitted from the PPC band structure for TM polarization and the upper omnidirectional band gap has been narrowed in comparison with MMPCs. Instead of the angular band gap in a MMPC, two branches of angular band gaps can be seen at different frequencies in the PPC, although the Bragg band gap branches are similar in both types of MMPCs and PPCs.

Figures 3(b) and 4(b) for the case of band structures related to TE polarization show that, like TM polarization, the lower omnidirectional band gap in the PPC has disappeared in comparison with MMPCs and the upper omnidirectional band gap has narrowed, although the angular and Bragg band gaps are approximately similar in both crystals.

For the type 2 PCs seen in Figs. 5(a) and 7(a), for TM polarization,the band gap width related to the "zero averaged refractive index" of the PPC, unlike the MMPC, has remained constant as the angle increases. The band gap width for "zero permittivity" has increased in comparison with MMPCs. The width of the Bragg band gap branch of the PPC has narrowed and shortened.

For TE polarization in PPCs, as seen in Figs. 5(b) and 7(b), two branches of band gaps known as "zero averaged refractive index" and 'zero permeability" have widened and are connected in comparison with MMPCs, although the Bragg band gap has narrowed and shortened.

4. Conclusions

To summarize, the band structure of two types of MMPCs and PPCs are plotted in order to compare 1DMMPCs with 1DPPCs using the Fresnel coefficients and transfer matrix methods. A comparison of the results of these methods can be seen in Figs. 3(a)–7(b).

It can be seen that the results of the two methods are the same and overlap. The band structures of the PPCs differ from the MMPC's because the permittivity of the plasma

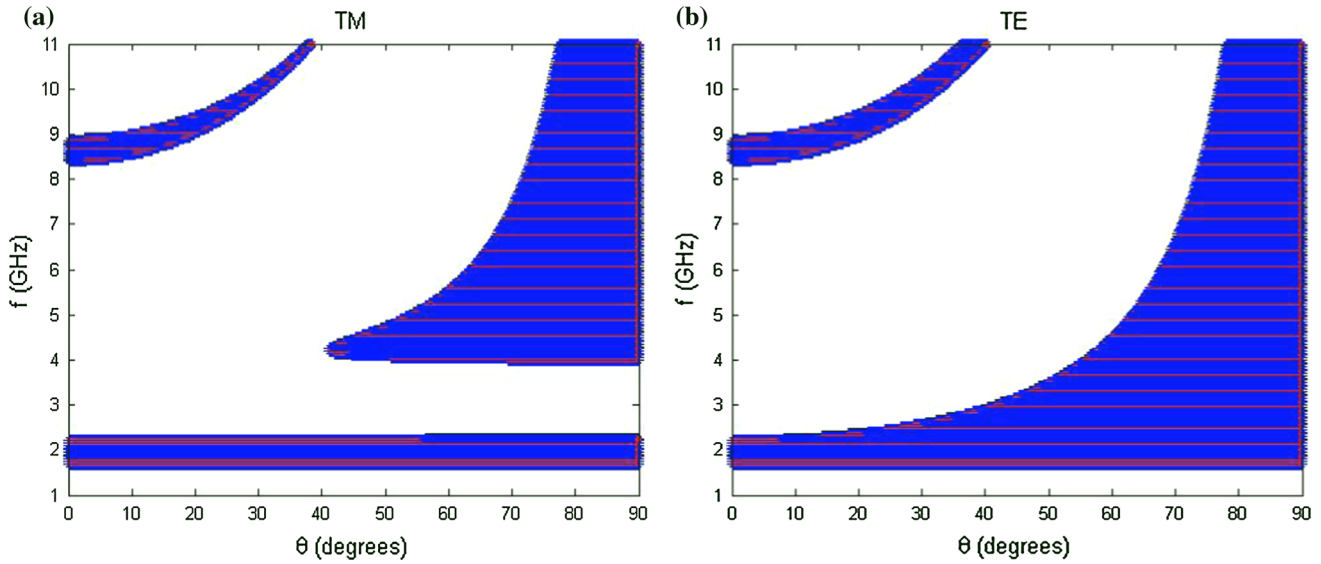

Fig. 7 Band structure of type 2 PPCs by Fresnel coefficients method (*blue color*) and transfer matrix method (*red color*) for: (**a**) TM polarization and; (**b**) TE polarization (color figure online)

layer is dependent on the incident field frequency, which obeys the Drude model.

In the type 1 MMPCs, electric permittivity of the second layer of dielectric is dependent on the incident field frequency, which is not compatible with the Drude model for PPCs. In addition, the band gap diagrams for high frequencies are identical to the corresponding PPC diagrams for both TE and TM polarizations, while differences are observed for both polarizations at low frequencies. For type 2 PCs, the permittivity and permeability of the second layer are dependent on the incident field frequency, which differs from the Drude model. The band gap diagrams of type 2 MMPCs and PPCs for both TE and TM polarizations are completely different. These different properties lead to a wide range of applications for PPCs.

Acknowledgements This study was supported by Urmia University in Urmia, Iran (Grant No. 10.195).

References

[1] D Shir, E C Nelson, Y C Chen, A Brzezinski, H Liao, P V Braun, P Wiltzius, K H A Bogart and J A Rogers *Appl. Phys. Lett*. **94** 011101 (2009)
[2] M Araghchini *et al*. I Celanovic and J D Joannopoulos *J. Vac. Sci. Technol. B* **29** 061402-1 (2011)
[3] C C Cheng and A Scherer *J. Vac. Sci. Technol. B* **13** 2696 (1995)
[4] P R Villeneuve, S Fan, S G Johnson and J D Joannopoulos *IEE Proc. Optoelec* **145** 384 (1998)
[5] M E Walsh PhD Thesis (MIT, USA) (2004)
[6] L C Liang, W Tao and P J Xiong *optoelectron. Lett*. **6** 0363 (2010)
[7] M Upadhyay, S K Awasthi, L Shiveshwari, S N Shukla and S P Ojha *Indian journal of physics* **90** 353 (2016)
[8] A H AL-Janabi, H J Taher and S M Laftah *Indian journal of physics* **85** 1299 (2011)
[9] H Hojo, K Akimoto and A Mase Conference Digest on 28th Int. Conf. Infrared and Millimeter Waves (Otsu, Japan, Sept.28-Oct.2) 347 (2003)
[10] H Hojo, N Uchida, K Hattori and A Mase *Plasma and Fusion Research* **1** 021-1-2 (2006)
[11] G Guida, A de Lustrac and A priou *PIER* **41** 1 (2003)
[12] E Yablonovitch *Phys. Rev. Lett.* **58** 2059 (1987)
[13] S John *Phys. Rev. Lett*. **58** 2486 (1987)
[14] H Hojo and A Mase *plasma and fusion Research* **80** 89 (2004)
[15] J D Joannopoulos, S G johnson, J N Winn and R D Meade *photonic crystals: Molding the Flow of light* (USA: Princeton, Princeton University Press) *2nd Ed.* p 44 (2008)
[16] J N Winn, Y Fink, S Fan and J D Joannopoulos *Opt. Lett*. **23** 1573 (1998)
[17] B Guo *physics of plasmas* **16** 043508 (2009)
[18] B Guo *plasma Science and Technology* **11** 18 (2009)
[19] Z Wang and D Liu *Appl. Phys. B* **86** 473 (2007)
[20] B Guo and X M Qiu *Optik* **123** 1390 (2012)
[21] Z Y Li and L L Lin *Phys. Rev. E* **67** 046607 (2003)
[22] J J Wu and J X Gao *J Supercond Nov Magn* **27** 667 (2014)
[23] R A Depine, M L M Ricci, J A Monsoriu, E Silvestre and P Andres *Phys. Lett A* **364** 352 (2007)
[24] L G Wang, H Chen and S Y Zhu *Phys. Rev. B* **70** 245102 (2004)
[25] Y Fink, J N Winn, S Fan, C Chen, J Michel, J D Joannopoulos and E L Thomas *Science* **282** 1679 (1998)
[26] M Mansuripur *Opt.& Phot. News* **9** 8 (1998)
[27] M Born and E Wolf *Principles of Optics* (England: Cambridge, Cambridge University Press) *7th Ed.* p 38 (1999)
[28] J B Pendry, A J Holden, W J Stewart and I Youngs *Phys. Rev. Lett*. **76** 4773 (1996)
[29] V G Veselago *Sov. Phys. Usp*. **10** 509 (1968)
[30] D R Smith, W J Padilla, D C Vier, S C Nemat Nasser and S Schultz *Phys. Rev. Lett*. **84** 4184 (2000)
[31] D R Smith and N Kroll *Phys. Rev. Lett*. **85** 2933 (2000)
[32] A L Pokrovsky and A L Efros *Phys. Rev. Lett*. **89** 093901 (2002)
[33] J Li, L Zhou, C T Chan and P Sheng *Phys. Rev. Lett*. **90** 083901 (2003)

[34] H Jiang, H Chen, H Li, Y Zhang and S Zhu *Appl. Phys. Lett*. **83** 5386 (2003)
[35] H F Zhang, S B Liu, X K Kong, L Zou, C Z Li and W Qing *physics of Plasmas* **19** 022103 (2012)
[36] H Jiang, H Chen, H Li, Y Zhang, J Zi and S Zhu *Phys. Rev. E* **69** 066607 (2004)
[37] N Garcia, E Ponizovskaya and J Xiao *Appl. Phys. Lett*. **80** 1120 (2002)
[38] B Schwartz and R Piestun *J. Opt. Soc. Am. B* **20** 2448 (2003)